Proceedings of Ninth World Conference on Earthquake Engineering
August 2-9, 1988, Tokyo-Kyoto, JAPAN (Vol.II)

3-7-11

SIMULATION OF THE GROUND MOTION AT KALAMATA CITY - GREECE

Nikolaos THEOFANOPOULOS[1] and Kazuo DAN[2]

[1]Department of Architecture, University of Tokyo Metropolitan,
2-1-1 Fukazawa, Setagaya-ku, Tokyo 158, Japan

[2]Ohsaki Research Institute, Shimizu Corporation, Fukoku Seimei Bld.,
2-2-2 Uchisaiwaicho, Chiyoda-ku, Tokyo 100, Japan

SUMMARY

On September 13, 1986 a strong earthquake (Ms=6.2) hit the city of Kalamata, Southern Greece, resulting in collapse or heavy damage of a large number structures. The earthquake occurred at a shallow focal depth, near the Kalamata city, producing a maximum intensity of MM VIII in the center of the city and MM X at the village of Elaiochori, 10 km east of Kalamata city, where all but three of 120 homes have been destroyed. In the present research, besides the study of some earthquake characteristics, the ground motions for the main shock have been simulated. The simulations have been performed at Kalamata city by synthesizing the aftershock records and at Elaiochori village by considering the attenuation due to the distance and the amplification due to the response of the mountain where the village is located.

INTRODUCTION

The Kalamata earthquake (Ms=6.2) and its strongest aftershock (Ms=5.4) are the subject of the present strong motion analysis. The main shock of the earthquake was a shallow event (Depth=6.2 km) in the overriding continental crust of the Aegean. The strong motion accelerograms recorded within 15 km of the rupture zone were analyzed. The strong motion records obtained during the main shock and the major aftershock were digitized, base-line corrected and band-pass filtered. The time variation of frequency components of the recorded accelerograms was examined by means of evolutionary power spectral analysis (Ref. 1). To understand the fault rupture procedure, principal axes analysis (Ref. 2) using moving window techniques has been carried out. Furthermore, a new synthesis method was applied to simulate the ground motion during the main shock by the use of the aftershock records as Green functions. In the case of synthesis of ground displacement or velocity motions, the number of superposition of the aftershock records is basically the ratio of the seismic moment between the aftershock and the main shock (Ref. 3) but in the case of synthesis of acceleration motions, more attention must be paid to the efficiency of generation of short period motions which does not correspond directly to the seismic moment (Ref. 4,5). In this paper, the source spectra for both events were modeled by the approximate source spectrum proposed by Brune (Ref. 6), in which the difference of the long period motions between the two events was taken into account by considering the seismic moment, and that of the short period motions by considering the effective stress and the fault area.

ANALYSIS OF THE RECORDS

Two main shock and three aftershock near field strong motion records were obtained at the existing stations of National Observatory of Athens (NOA) and Greek Institute of Engineering Seismology and Earthquake Engineering (ITSAK). The location of the stations, the epicenters of the main shock and the aftershocks, as well as, the surface breaks from the recent earthquakes are shown in Fig.1.

Large horizontal peak accelerations were observed for the main shock, as well as, for the major aftershock. The vertical peak acceleration of the main shock (368.6 gal) exceeded the horizontal ones (292.1 and 221.8 gal) at OTE1 station of NOA. Significantly large horizontal spectral acceleration values have been observed for periods between 0.2 and 0.8 sec. (Ref. 7). The dynamic characteristics of the most of the structures in the city are within the above period range. The root-mean-square accelerations take high values due to the short duration of the intense part of the records.

Two-dimensional (horizontal plane) principal axes analysis over the total duration for both main shock and aftershock records has been employed. In Fig.2 is shown the direction of the major principal axis for the main shock (station OTE1) and the aftershock (station OTE2) in relation to the directions along which the instrumental records were obtained. The general direction to the epicenter is also plotted. Judging from this figure, the major principal axis points to the epicenter. Fig.3 shows the time-dependent principal axes variations for the same records, resulted from principal analysis using moving average with time span of 2 sec.. The solid and dashed lines represent the major and intermediate axes respectively. From this figure a total directional variation of about 90 degrees during the strong motion interval can be observed in the case of the main shock. Assuming that the direction of the major principal axis coincides with the direction to the energy release zone in the fault plane, it can be concluded that the rupture propagates approximately from North to South along the Kalamata fault. The rupture starts approximately to the North and ends to the North-East by East of Kalamata city. On the other hand, the direction of the major principal axis for the major aftershock remains considerably constant during the intense motion interval, indicating obviously a localized rupture along the Kalamata fault.

Moreover, the evolutionary power spectra of the strong motion accelerograms have been obtained. In Fig.4 is shown an example of the evolutionary power spectrum for the vertical component of the major aftershock recorded at OTE2 station. Dispersive characteristics can be observed at the frequency range between 0.60 and 1.15 Hz. After careful examination of the evolutionary spectra for the horizontal components of both main shock and aftershock, recorded at Kalamata city, can be observed slow traveling wave trains which arrive with delay to the stations, but they can not be classified clearly as surface or multi-path body waves. For the recordings of the major aftershock at Messini city (MES), dispersive characteristics can be observed clearly for all three components.

SYNTHESIS OF THE MAIN SHOCK AT KALAMATA CITY

The theoretical background of the method is explained at (Ref. 8, 9). After careful examination of the distribution of the aftershocks in Fig.1, it can be concluded that there are two clusters of seismic activity separated by a gap, where low aftershock activity was recorded. The epicenter of the main shock was placed (Ref. 10) at the Northern cluster and for the major aftershock at the

Southern cluster. The fault extend for the main shock was unknown, for this reason two different fault planes, with dimensions 14x14 Km^2 and 7x14 km^2 respectively, have been assumed. The surface projections of these models are shown in Fig. 5. The first assumption corresponds to the rupture of the entire aftershock zone and the second one to the rupture of the Northern cluster only. The dislocation was assumed to be equal to 15 and 30 cm respectively, in order to assure a constant seismic moment (Mo) value for both models. The strike, dip and slip angles for the fault plane of the main shock were taken equal to 203, 45 and -77 degrees respectively. The other parameters used for the simulation are summarized in Table 1. The ratios of the ruptured length (L), width (W), average dislocation (D) and effective stress (σ_e) of the main shock to those of the major aftershock were assumed to be equal to 3, 3, 3 and 1 respectively, based on the similarity relations of the earthquakes proposed in (Ref. 11). At Nomarchia station (NOM) of ITSAK, both main shock and aftershock records were available. By the use of the aftershock records as Green functions, the main shock was synthesized for both fault models. In Fig.6 are shown (a) the aftershock motion (N80E), (b) the synthesized motion for the first assumption (whole fault), (c) the synthesized motion for the second assumption (Northern cluster) and (d) the main shock motion (N80E). In the case of the first assumption (whole fault) the simulation of both envelope of the motion and strong motion duration was fairly good but the error for the peak acceleration was about 49.5%. In the case of the second assumption (Northern cluster) the wave form, the amplitude and the duration time of the strong motion were simulated well. This result lead us to the conclusion that the second assumption was more realistic. Fig.7 shows the comparison between the velocity response spectra of the recorded and the synthesized motions for the main shock. The solid line is for the observed motion and the dotted lines are for the synthesized motions. A good agreement can be observed between the spectral curves of the recorded motion and the synthesized one for the second assumption (Northern cluster).

SYNTHESIS OF THE MAIN SHOCK AT ELAIOCHORI VILLAGE

In order to explain the extended damages at Elaiochori village, which is located on a mountain at height of 525 m, the following method was adopted. The acceleration motions for the aftershock recorded at NOM station by the use of body waves attenuation have been transferred to the base of the mountain where Elaiochori village is located. By the use of these motions as Green functions, the main shock was synthesized. The second assumption for the fault model (Northern cluster) has been adopted. The synthesized motions for N80E and N10W directions were transformed to the principal axes. The major principal axis of the synthesized motion is shown in Fig.8.

The mountain where the Elaiochori village is located was modeled (Fig.9) as a linearly elastic shear beam with an exponentially varying cross-section (Ref. 12). Since the height-to-width ratio of the mountain is small, it can be assumed that the primary response of the mountain will be mostly in shear and the effect of bending on its response will be negligible. The ratio of the area of the top cross section of the mountain to that of the base was assumed equal to 0.03, the shear wave velocity equal to 2000 m/sec., the height to the top of the hill equal to 742 m and the height where Elaiochori village is located equal to 525 m. The analysis was based on the first 8 modes. The resulted motion at the height of 525 m is shown in Fig.10. The acceleration response spectrum of the motion at the base of the hill and that of the motion at Elaiochori village are shown in fig.11. It can be observed a great amplification of the motion for the period range between 0.3 and 1.6 sec.. The buildings in Elaiochori village were generally one or two-story old houses with masonry walls made of stones or bricks without any antiseismic provisions. Some of the houses were made of

reinforced concrete with unreinforced brick walls used as partitions. This kind of structures was completely inadequate to withstand such a high level of earthquake forces introduced during the main shock.

CONCLUSIONS

The extended damages in Kalamata city can be attributed to the high spectral values at frequency range that corresponds to the dynamic characteristics of the existing structures. The existence of surface waves in some records was verified by evolutionary spectral analysis. The rupture propagation during the main shock was examined by means of moving window principal axes analysis. It was verified that the rupture starts approximately to the North of Kalamata and ends to the North-East by East of the city. The fault model synthesis used for the simulation of the main shock by the use of the aftershocks as Green functions, was proved powerful enough, resulting to realistic values of peak acceleration, strong motion duration, predominant frequency and response spectra in good agreement to those of the recorded motions. Only the Northern cluster of Kalamata fault must have been ruptured during the main shock because this assumption resulted in a synthesized motion with similar characteristics to the recorded one. The extended damages that observed at Elaiochori village can be explained well by the high acceleration spectral values at the period range between 0.15 and 1.6 sec calculated by the use of the synthesized earthquake motion.

REFERENCES

1. Kameda, H., "Evolutionary Spectra of Seismogram by Multifilter", Journal Eng. Mech. Division, ASCE, 101, EM6, 787-801,(1980).
2. Penzien, J. and Watabe, M., "Characteristics of 3-Dimensional Earthquake Ground Motions", Earthquake Eng. Struct. Dynamics, 3, 365-373, (1975).
3. Irikura, K., "Semi-empirical Estimation of Strong Ground Motions during Large Earthquakes", Bull. of Disaster Prevention Research Institute, Kyoto Univ., 33, Part 2, No. 298, 63-104,(1983).
4. Irikura, K., "Prediction of Strong Acceleration Motions using Empirical Green's function", Proc. 7th Japan Earthquake Eng. Symp., 151-156, (1986)
5. Takemura, M. and Iekura, T., "Semi-empirical Synthesis of Strong Ground Motions for the Description of Inhomogeneous Faulting", Zishin, 40, No.2, 77-88, (1987).
6. Brune, J., "Tectonic Stress and the Spectra of Seismic Shear Waves from Earthquakes", Journal of Geophysical Research, 75, No.26, 4997-5009, (1970)
7. Anagnostopoulos, D., Rinaldis, D., Lekidis, V., Margaris V., Theodulidis, N. "The Kalamata, Greece, Earthquake of September 13, 1986",Earthquake Spectra, 3, No.2, 365-402, (1987).
8. Dan, K., Watanabe, T., Tanaka, T., "Synthesis of Earthquake Ground Motions Based on Approximate Spectrum for Far-field Shear Wave and Scaling Law of Earthquakes", Proc. of the Annual Meeting of Architectural Institute of Japan, (In Japanese), (1987).
9. Theofanopoulos, N. and Dan, K., "Generation of Input Earthquake Motions for Disaster Countermeasures", Proc. of the International Symposium on Earthq. Countermeasures, Beijing, China, (1988).
10. Papazachos, B., Kiratzi, A., Karakostas, B., Panagiotopoulos, D., Scordilis, E., "Surface Fault Traces, Fault plane solution and Spatial Distribution of the Aftershocks of the September 13, 1986 earthquake of Kalamata", Preprint.
11. Kanamori, H. and Anderson, D., "Theoretical Basis of some Empirical Relations in Seismology, BSSA, 65, No.5, 1073-1095,(1975).
12. Theofanopoulos, N., Watabe, M., Hanazato, T., "Strengthening of Parthenon Against Earthquake Motions-Part 2 Input Earthquake Motions", Proc. of the Annual Meeting of Architectural Institute of Japan, (In Japanese),(1988).

Characteristics		Main Shock	Aftershock
Latitude		37.110° N	37.040° N
Longitude		22.140° E	22.130° E
Focal depth		6.2 km	4.0 km
Magnitude	(Ms)	6.2	5.4
Fault length	(L)	14. 7 km	4.7. 2.3 km
Fault width	(W)	14 km	4.7 km
Dislocation	(D)	15. 30 cm	5. 10 cm
Seismic moment	(Mo)	8.8×10^{24} dyne.cm	3.3×10^{23} dyne.cm
Effective stress	(σe)	30 bar	30 bar
Corner frequency	(ωc/2π)	0.277 Hz	0.832 Hz
Distance	(r)	11.1 km	4.4 km
		Common Parameters	
Rigidity	(μ)	3×10^{11} dyne/cm^2	
Shear wave velocity	(β)	3 km/sec	
Density	(ρ)	3.3 g/cm^2	
Quality factor	(Q)	200	

Table 1. Source parameters for the 1986 Kalamata earthquake.

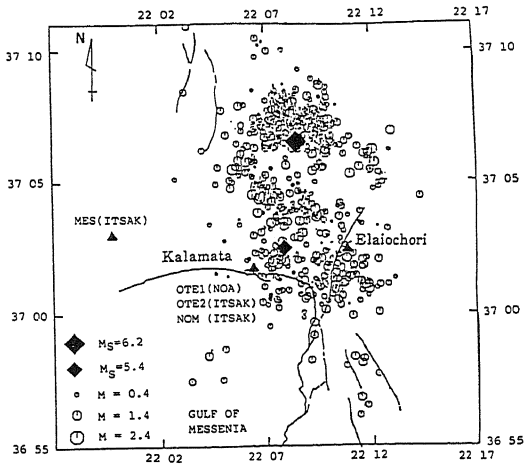

Fig. 1. Strong motion accelerograph stations location, epicenters for the main shock and the major aftershock and distribution of aftershocks.

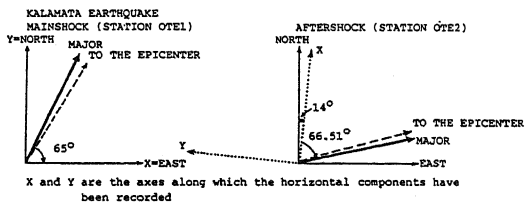

Fig. 2. Major principal axis direction (Total duration)

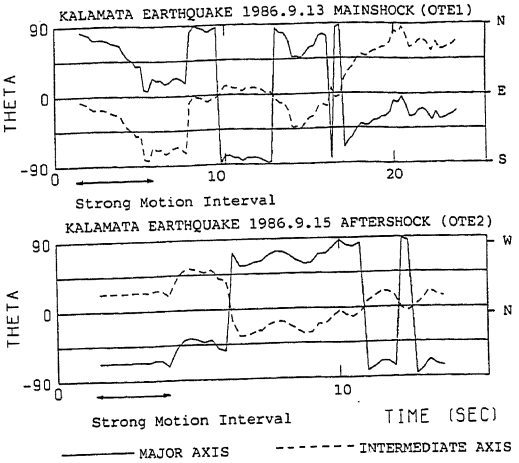

Fig. 3. Principal axes direction (Moving average)

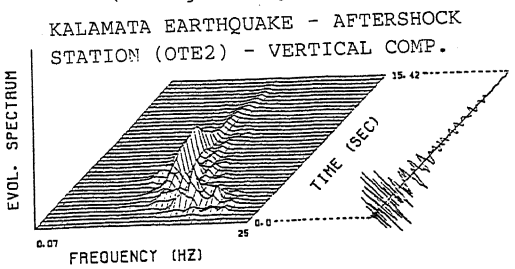

Fig. 4. Evolutionary Power Spectrum with damping 0.05%.

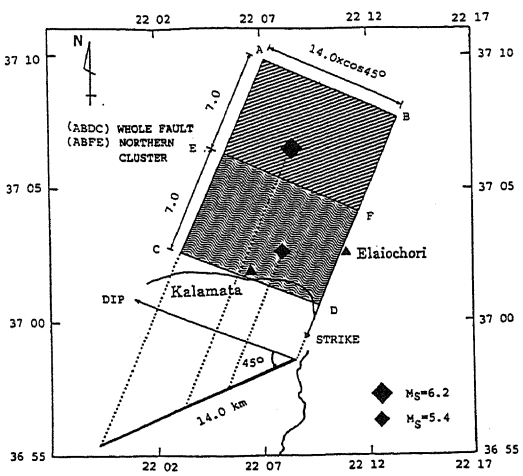

Fig. 5. Fault model for the synthesis of the main shock.

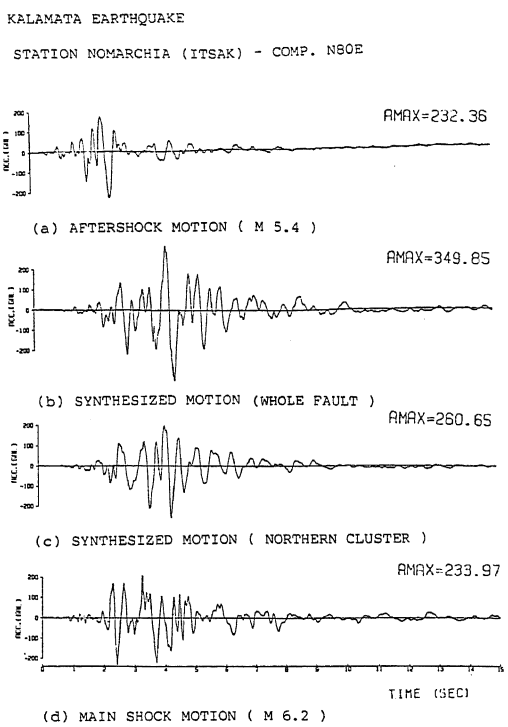

Fig. 6. Comparison of the observed and the synthesized motions at Nomarchia (NOM) station.

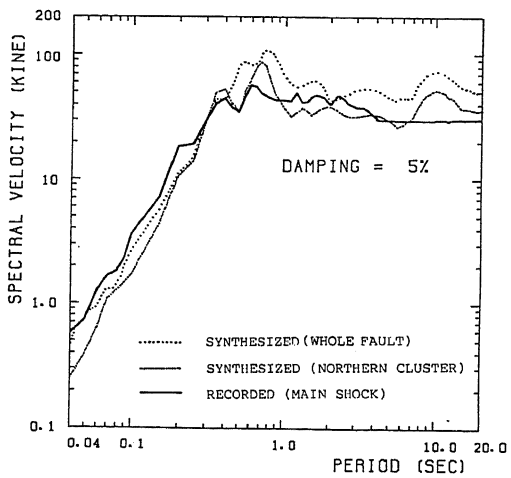

Fig. 7. Comparison of the response spectra of the acceleration motions (b),(c),(d) in fig. 6.

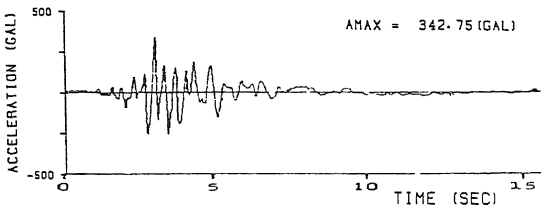

Fig. 8. Major principal axis of the synthesized motion at the base of the mountain.

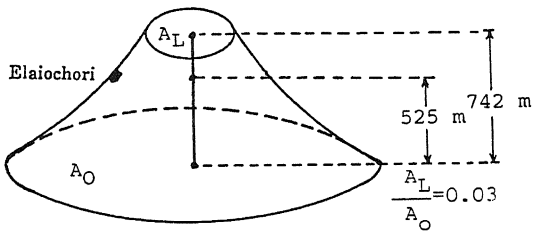

Fig. 9. The mountain model and its parameters.

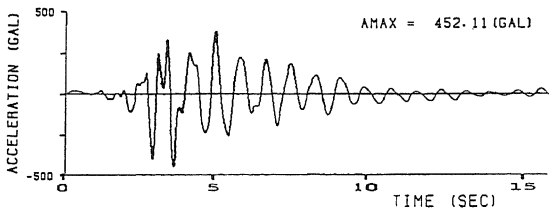

Fig. 10. Acceleration motion at Elaiochori village (Main shock).

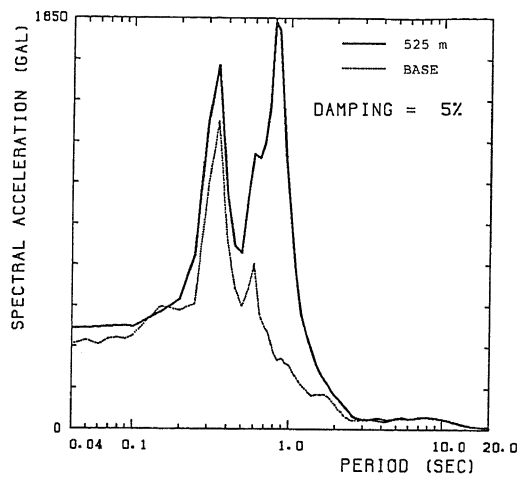

Fig. 11. Comparison of the response spectra of acceleration motions in figures 8 and 9.